Neural Network-Based Electric Vehicle Range Prediction for Smart Charging Optimization

Matthew J. Eagon[*†‡]
Graduate Research Assistant
University of Minnesota Twin Cities
Minneapolis, Minnesota 55455
Email: eagon012@umn.edu

Daniel K. Kindem[†]
Graduate Research Assistant
University of Minnesota Twin Cities
Minneapolis, Minnesota 55455
Email: kinde064@umn.edu

Harish Panneer Selvam[†]
Graduate Research Assistant
University of Minnesota Twin Cities
Minneapolis, Minnesota 55455
Email: panne027@umn.edu

William F. Northrop[†]
Associate Professor
Director, T. E. Murphy Engine Research Lab
University of Minnesota Twin Cities
Minneapolis, Minnesota 55455
Email: wnorthro@umn.edu

Range prediction is a standard feature in most modern road vehicles, allowing drivers to make informed decisions about when to refuel. Most vehicles make range predictions through data- or model-driven means, monitoring the average fuel consumption rate or using a tuned vehicle model to predict fuel consumption. The uncertainty of future driving conditions makes the range prediction problem challenging, particularly for less pervasive battery electric vehicles (BEV). Most contemporary machine learning-based methods attempt to forecast the battery SOC discharge profile to predict vehicle range. In this work, we propose a novel approach using two recurrent neural networks (RNNs) to predict the remaining range of BEVs and the minimum charge required to safely complete a trip. Each RNN has two outputs which can be used for statistical analysis to account for uncertainties; the first loss function leads to mean and variance estimation (MVE), while the second results in bounded interval estimation (BIE). These outputs of the proposed RNNs are then used to predict the probability of a vehicle completing a given trip without charging, or if charging is needed, the remaining range and minimum charging required to finish the trip with high probability. Training data was generated using a low-order physics model to estimate vehicle energy consumption from historical drive cycle data collected from medium-duty last-mile delivery vehicles. The proposed method demonstrated high accuracy in the presence of day-to-day route variability, with the root-mean-square error (RMSE) below 6% for both RNN models.

[*]Corresponding author
[†]Department of Mechanical Engineering
[‡]Department of Computer Science & Engineering

Nomenclature

Acronyms

BEV	Battery electric vehicle
BIE	Bounded interval estimation
FNN	Feedforward neural network
HEV	Hybrid electric vehicle
ICEV	Internal combustion engine vehicle
MPC	Model predictive control
MPIW	Mean prediction interval width
MVE	Mean variance estimation
PHEV	Plug-in hybrid electric vehicle
PICP	Prediction interval coverage probability
RMSE	Root Mean Square Error
RNN	Recurrent neural network
SOC	Battery pack average state of charge

Definitions

α	Upper bound on points outside predicted bounds	–
β	Minimum probability of finishing the trip with C	%
η_r, η_{btw}	Recapture & battery-to-wheel efficiency	–
λ	Hyperparameter/lagrange multiplier	–
μ, σ	Mean & standard deviation of SOC_{togo} prediction	%
a	Vehicle acceleration	m/s
C	SOC recaptured from charging	%
d	Traveled trip distance	mi
d_{rem}	Estimated remaining trip distance	mi
d_{trip}	Total distance covered by the trip	mi
I	Current driven through load by battery	A
i	Time step index	s
j	Earliest timestep when SOC falls below SOC_{min}	s
P_b	Power delivered by traction battery	W
P_d	Power demand	W

P_r	Regenerative braking power	W
R_0	Battery internal resistance	Ω
R_{pred}	Predicted remaining driving range	mi
V_{oc}	Battery open-circuit voltage	V
SOC_{des}	SOC_{req} assuming data is normally distributed	
SOC_{min}	Minimum allowable SOC for safe discharge	%
SOC_{req}	SOC required to complete the trip with SOC_{min}	%
SOC_{togo}	Expected SOC required to complete the trip	%
$SOC_{up/lo}$	Predicted upper/lower bounds for SOC_{togo}	%

1 Introduction

As the world transitions from fossil fuel-powered vehicles to electric ones through the development of higher capacity batteries, better charging infrastructure, and policy interventions, some factors still stand as obstacles for consumer acceptability. Electric trucks are starting to be preferred over diesels due to their lesser environmental impact and more energy efficient operation [1]. Range anxiety, or the fear of one's vehicle having insufficient range to reach the intended destination, is one of the largest barriers for new BEVs purchases in the US [2]. This problem is especially exacerbated for long distance trips, where electric charging stations on the driving path are more scarce than in urban areas.

A reliable understanding of the vehicle's range can reduce driver range anxiety significantly. A study in the UK found that on-board range estimation of most EVs currently on the road may be more than 100 percent inaccurate [3]. Range prediction is a difficult problem because estimations vary appreciably based on ambient temperature, driving style and traffic conditions among other factors. Limited information about future paths of the vehicle is a hurdle to overcome when accurate prediction of the remaining driving range is desired. However, a probabilistic estimate of whether a vehicle completes the trip or otherwise based on historical driving data, vehicle energy consumption, and source-destination specification is a more pragmatic and helpful way of looking at range for the everyday vehicle user and fleet operators. The expected energy required to complete the intended trip and learning when to charge are important pieces of information for a BEV driver.

Using historical driving cycles and energy information as inputs, classical range prediction solutions are tasked with predicting the distance a vehicle is expected to be able to travel with the remaining fuel. If an energy-centric view is taken instead, the range prediction problem may be modified to predict the expected energy needed to complete a given trip. A distance prediction may then be obtained by comparing the expected energy needed with the remaining available energy. The energy-centric view may help improve range prediction by considering each trip separately since driving conditions can vary along a single route and routes can change day-to-day.

The method proposed in this work uses two recurrent neural networks (RNNs) to make parallel predictions about the energy required to complete the current trip. Using a tuned vehicle model, historical driving data is transformed into labeled training data in the preprocessing step. The first RNN is trained to perform mean-variance estimation (MVE) assuming a normal distribution for the output. The mean output is the expected state of charge (SOC) needed to complete the trip, and the variance gives a measure of the prediction confidence. The second RNN is trained to perform bounded-interval estimation (BIE), outputting the expected upper and lower bounds for the SOC required to complete the trip. These model outputs are then used to predict the expected probability of completing the trip with a known minimum SOC, the minimum charging required to increase the probability of finishing the trip above some minimum threshold, and the expected remaining range of the vehicle.

Due to the temporal auto-correlation associated with driving data, RNNs are a more natural problem solution for range prediction than ordinary feedforward neural networks (FNNs). While neural networks are often criticized as black-box models that have little physical interpretability, they can often provide highly accurate results even in the presence of nonlinearities. In the proposed solution, the RNN outputs are easily interpretable, providing tunable statistical bounds on the expected energy required to complete a trip, and are informed by a glass-box physics model preprocessing the raw drive cycle data.

The MVE and BIE RNNs proposed in this work have not previously been used to solve the target problem. These models have the advantage of providing tunable confidence measures on their predictions, which allow the subsequent probability of finishing the trip and minimum required charge estimates to include known levels of certainty. Additionally, by estimating the SOC required to complete the trip rather than the SOC discharge profile for a single vehicle, these models have strong potential to generalize their predictions well for different drive cycles. The methods developed for estimating the minimum charging required to complete the trip and the expected vehicle range are also novel. The battery state of health (SOH) is often protected by bounding the upper and lower SOC limits to avoid overcharging and over-discharging. If the choice of minimum SOC and/or the minimum charging estimates are not conservative, the risk of over-discharging could be detrimental to the battery SOH. The proposed minimum required charging estimation relies on the statistical confidence of a vehicle's ability to finish the trip above a specified minimum SOC, allowing for conservative charging estimates that ensure vehicle safety and battery health with high probability. For the range prediction problem, the trip-centric view provides a lower-bound range estimate since BEVs often are able to recharge at the end of each trip. Therefore, BEV owners often only need to know whether they will complete the current trip or not before needing to charge. If the trip range exceeds the maximum vehicle range, this lower-bound estimate becomes an exact range estimate.

This new technique for parameter estimation has potential to be leverage by both BEV drivers and future autonomous BEV control systems, and may be used in conjunction with other methods from dynamics and control or artificial intelligence to develop systems with sophisticated decision making capabilities. Notably, neural network-based model predictive control (MPC) and sliding mode adaptive control techniques have been explored in many recent works. For example, an RNN-based MPC approach was presented by Zhang et al. for multi-vehicle formation tracking with autonomous quadrotor aerial vehicles [4]. Neural networks have also been used in a number MPC-based energy management strategies, primarily to make fast predictions over the chosen horizon period. Two newer examples include the strategies adopted by Wu et al. and Hu et al. for plug-in hybrid electric vehicles (PHEVs) and hybrid electric vehicles (HEVs), respectively. [5, 6]. Wu et al. used multiple neural networks for mode, co-state, and velocity prediction [5], while Hu et al. utilized a single neural network to make medium-range vehicle speed predictions [6].

This work makes a significant contribution to the field of intelligent energy management of electric vehicles. It provides a novel method for estimating key values, like energy required to complete a trip, that are not directly measurable but are helpful to BEV drivers and fleet managers. The presented implementation makes some simplifications, such as assuming a Gaussian distribution for the underlying data and testing on data from delivery vehicles assumed to have somewhat regular drive cycle patterns, but the overall framework is more general and adaptable to different cases.

2 Literature Review

In the literature, electric vehicle range prediction has been explored through either physical models based on instantaneous information or artificial intelligence models trained on historical vehicle data. Physical models may further be classified by energy consumption estimation through modeling either the battery pack (or powertrain) or the vehicle itself.

Examples of a battery pack models include using the apparent state of discharge of the Li-ion cells adjusted for the effects of current and temperature [7], and using online battery identification parameters to update a battery dynamics model [8]. Battery-in-loop simulations have been used effectively in analyzing energy consumption in cold temperatures [9]. Drive cycle data for specific scenarios like coast-down have been used to develop simplified powertrain models [10]. Battery pack models are especially effective in accounting for the energy usage by auxiliary vehicle loads and its dependence on ambient temperature [11]. Vehicle models include using physical parameters such as velocity, road inclination, vehicle mass [12, 13] that can provide statistical information about a BEV's instantaneous energy consumption. Future energy consumption has been predicted using additional road information to compare results between faster driving speed and the most economical driving speed [14]. Though these methods are accurate with known data about the future route or drive cycle, they are not able to predict energy for the remaining part of a trip without future information.

Studies have identified driving style as the most influential factor in variable BEV range [15]. Due to this reason, historical vehicle data is required to estimate the remaining driving range. Range prediction is a complex problem that is affected by internal and external, as well as constant and variable parameters [16, 17]. Big-data models have been used for predicting range using numerous data sources [18]. Most works in the literature using artificial intelligence models have combined historical vehicle data and its attributes coupled GIS-based information [19] and other external parameters like road conditions and traffic [20]. Optimal path search algorithm-based predictive strategy for BEV range [21], multi-objective optimization problems with recommended vehicle speeds [22], and machine learning models based on trip data [23, 24] are other data-driven approaches to estimating BEV range. Some methods have other attributes such as tire-pressure monitoring combined with a physical energy consumption model to estimate range [25]. More recent studies have used powerful machine learning techniques such as XGBoost and LightGBM methods along with features such as motor and battery energy, driving patterns, and battery temperature to obtain range of BEVs [26]. Least square support vector machine models combined with particle swarm optimization have also been used by training on features like temperature and depth of discharge to obtain stable and reliable range prediction [27].

Black-box neural networks are known to generally offer more accurate predictions when compared to more interpretable machine learning regression models [28]. One study transformed driving cycles to 1D and 2D static maps that were used as input to deep neural networks to output energy demand and BEV range [29]. Hybrid convolutional neural networks and bagged decision trees have also been used to estimate energy consumption from features like temperature, wind speed, and battery SOC [30]. A probability distribution of the remaining driving range obtained from a Markov chain model with particle swarm optimization is one effective way of looking at this problem [31], and is similar to the one described in this study. Previous works using methods similar to the proposed MVE RNN [32] and BIE RNN [33, 34] for various applications are provided in the references and helped to inspire the proposed approach.

3 Problem Description

The goal of estimating the energy required to complete a trip for a BEV is two-fold: determining expected range and minimizing on-route charging if the vehicle is unlikely to finish the trip without charging. Contemporary methods typically predict the remaining range of a BEV by estimating the state of charge (SOC) discharge profile forward in time until it reaches some minimum threshold. Such methods allow for range predictions to be made beyond the trip at hand, but often rely on an abundance of historical driving data from the vehicle in which they are deployed, and tend to be less accurate for vehicles with inconsistent driving patterns. Instead, a trip-based view can be taken in which the main goal becomes determining how likely it is that a vehicle will need to charge, and if so, how much, during each individual trip. This revised formulation suits BEVs in particular since they are generally used to make short regular trips and charge at trip endpoints whenever possible. Therefore, in addition to directly predicting the vehicle SOC over time, the goal of this work is to determine the expected energy required to complete

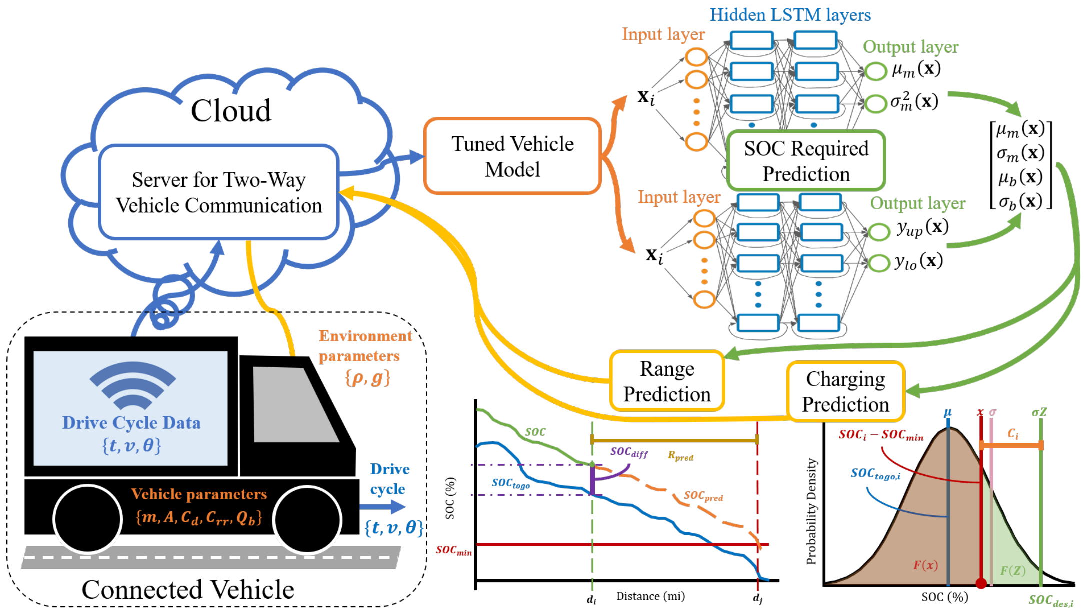

Fig. 1: The framework of the proposed method. Vehicle driving data, preprocessed via a vehicle model, is fed into the parallel RNNs, the outputs of which are used to predict the charging requirements and remaining range of the vehicle. Connected vehicles with two-way communication may then leverage this information from the model to make decisions.

the current trip. This has the advantage of better prediction generalization to different drive cycles and lengths as it avoids overfitting to one particular vehicle's driving patterns.

Given some general drive cycle data from a group of vehicles, the objective of the target problem as presented in Eq.(1) is to determine the minimum charge required for a BEV to complete a given trip with high confidence.

$$\begin{aligned} \min_{C} \|C\|_2^2 \quad \text{subject to } \mathbb{P}\left(SOC_i + C_i \geq SOC_{req,i}\right) \geq \beta \ \forall i \\ SOC_{req,i} = SOC_{togo,i} + SOC_{min} \end{aligned} \tag{1}$$

where C is the SOC recaptured from charging, SOC_{req} is the expected SOC required to complete the trip with at least SOC_{min} charge remaining, SOC_{togo} is the expected SOC required to complete the trip, and β is the minimum probability of finishing the trip with the current SOC_i and added SOC from charging C_i. Note that SOC_{req} is used in a general sense, without assumption on the underlying distribution. From here on, SOC_{des} is used in place of SOC_{req} because we specifically assume a Gaussian distribution for the underlying data to make the calculations in section 4.3.

Drive cycle data is assumed to include time series velocity, road inclination, and positioning (i.e. GPS latitude and longitude) measurements, collected at a reasonably high temporal resolution for the effective use of discrete numerical methods. Other optional attributes that impact energy usage such as vehicle mass, ambient temperature, etc. may also be utilized if available. A trained model should ideally make predictions quickly given limited information about the route. It is assumed that the intended route is known a priori, and therefore that the model may use an estimate of the remaining distance to travel. If the expected charging required is greater than zero, the range prediction problem is also solved by looking ahead to the point in time at which the current vehicle SOC relative to the expected SOC to complete the trip is equal to the minimum state of charge. This is described by Eq.(2).

$$\begin{aligned} R_{pred,i} &= d_j - d_i = d_{rem,i} - d_{rem,j} \\ SOC_{diff,i} &= SOC_i - SOC_{togo,i} \\ j &= \arg\min_{j} \ SOC_{diff,i} + SOC_{togo,j} \leq SOC_{min} \end{aligned} \tag{2}$$

where R_{pred} is the predicted remaining driving range of the vehicle (i.e. the remaining distance before the vehicle SOC is expected to reach SOC_{min}, the index i is used to denote the current timestep and index j is the first chronological timestep at which the forecast vehicle SOC discharge profile falls below SOC_{min}. d_{rem} is the estimated remaining trip distance. This gives theoretical bounds $R_{pred} \in [-d_{trip}, d_{trip}]$, where d_{trip} is the estimated total trip distance.

The proposed framework is summarized by Fig.1. Given historical driving data from a vehicle, and a tuned physical model for a similar BEV, the goal of the preprocessing step is to estimate energy consumption and arrange an input vector as a sequence of driving information for a single trip. This processed data is then passed into the RNNs to train. Once trained, the RNN models are used to predict the energy required to complete future trips. The outputs of the RNN model are then used to provide feedback to the vehicle operator about the probability of finishing the trip without charging, the minimum charging required to complete the trip, and the predicted remaining driving range (if on-route charging is required).

4 Methods

4.1 Vehicle Model

The tuned vehicle model for data preprocessing uses the simplified road load equation in Eq.(3), where energy information is estimated from the instantaneous power calculations.

$$P_d = \left[m\left(\frac{dv}{dt}\right) + mg\sin(\theta) + \frac{1}{2}\rho C_d A v^2 + mgC_{rr}\right] v \quad (3)$$

where P_d is the instantaneous power demand, m is the vehicle mass, v is the vehicle velocity, $a = (dv/dt)$ is the vehicle acceleration, ρ is the density of air, A is the frontal area of the vehicle, C_d is the drag coefficient, C_{rr} is the rolling resistance coefficient, g is the acceleration due to gravity, and θ is the road inclination angle.

The instantaneous demand from the road load equation Eq.(3) is met by the vehicle powertrain. In BEVs, the powertrain is typically much simpler than that of internal combustion engine-based vehicles (ICEVs) or hybrid electric vehicles (HEVs). The BEV powertrain typically includes battery packs, DC/DC converters, DC/AC converters, electric motors, and a transmission leading to the final differential gear that channels power to the wheels. It is common to lump losses from the battery-to-wheels into a single efficiency term encapsulating the average overall powertrain efficiency as given in Eq.(4).

$$\begin{aligned} P_b &= \frac{P_d - P_r}{\eta_{btw}} = \frac{\max(0, P_d) + \min(0, \eta_r P_d)}{\eta_{btw}} \\ &= V_{oc} I - R_0 I^2 \end{aligned} \quad (4)$$

where P_b is the power delivered by the traction battery, P_r is used to incorporate the effects of regenerative braking (i.e. when $P_d < 0$) with recapture efficiency η_r, and η_{btw} is the overall efficiency from battery to wheels. The battery pack itself may be modelled as a voltage source with internal resistance R_0 and open-circuit (e.m.f.) voltage V_{oc} driving a current I through the load.

Vehicle energy estimation is then possible through integration ($E_b = \int P_b dt$). The continuous-time battery pack average SOC dynamics are given by Eq.(5).

$$\dot{SOC} = -\frac{\int I dt}{Q_b} = -\frac{V_{oc} - \sqrt{V_{oc}^2 - 4R_0 P_b}}{2Q_b R_0} \quad (5)$$

where $\dot{SOC}$ is the rate of change of SOC as a function of time and Q_b is the nominal battery capacity. SOC serves as an estimate of the remaining usable energy divided by the total usable energy at full charge.

In the preprocessing step, drive cycle data as defined in Section 3 was used to estimate the SOC and remaining energy over time for a medium-duty BEV model. Trip distance was estimated from the velocity trajectory. The SOC was then used to determine the SOC required to complete the current trip, which served as the labeled RNN model output or ground truth data for training and testing. The relevant model parameters used to simulate the BEV behavior are listed in Tab.1.

Table 1: Vehicle model parameters

Parameter	**Definition**	**Value**	**Units**
ρ	Density of air	1.20	kg/m^3
A	Frontal area	10	m^2
C_d	Coefficient of drag	0.5	–
C_{rr}	Rolling resistance coefficient	0.005	–
g	Acceleration due to gravity	9.81	m/s^2
m	Vehicle mass	8000	kg
Q_b	Nominal battery capacity	96	kWh

4.2 Recurrent Neural Network Models

Long short-term memory (LSTM) layers were first proposed by Sepp Hochreiter et. al. [35]. LSTM layers offer a favorable alternative to simple RNN layers, which suffer from the vanishing gradient problem encountered by deep networks [36]. The proposed networks utilize the a stacked LSTM structure, wherein the sequence of hidden state outputs from the first LSTM layer are passed to the next hidden LSTM layer as inputs. This architecture, similar to the stacked RNN explained by Pascanu et. al. in [37], was analyzed in previous works by Alex Graves et. al. [38, 39] and used by others more recently [40, 41]. The networks in Fig.2 were implemented in Python 3 with Keras using the TensorFlow 2 backend. The network weights and biases are denoted by θ, the input tensor is denoted by Θ, and the emboldened $\mathbf{x}_i$ or simply $\mathbf{x}$ are used interchangeably for a single input sequence. The specific data used to train and test the networks is described further in section 5.

Used in parallel, the two developed RNN models provide different methods for predicting the minimum charging required for a BEV to finish a trip. For each discrete time step, the MVE RNN predicts the mean and variance of the expected SOC needed to complete the trip under the assumption that the model output follows a normal distribution at each time step (i.e. that an 'average' trip exists from which other trips differ in a normally distributed manner). On the other hand, the BIE RNN provides statistical lower and upper bounds on the expected SOC needed to complete the trip without assumptions about the underlying distribution of the data. Each of these networks have the same overall structure as shown in Fig.2, with two hidden layers between the input and output layers. The neural network specifications are summarized in Tab.2. The loss functions for MVE and BIE are given below in Eq.(6) and Eq.(8), respectively.

$$\begin{aligned} L_{MVE} &= -\log \mathbb{P}_\theta(y|\, \mathbf{x}) \\ &= \frac{\log \sigma_m^2(\mathbf{x})}{2} + \frac{(y - \mu_m(\mathbf{x}))^2}{2\sigma_m^2(\mathbf{x})} + \lambda_{MVE} ||\theta||_2^2 \end{aligned} \quad (6)$$

where μ_m and σ_m are the predicted output mean and variance of the distribution for some neural network weights and biases θ. Note that L_{MVE} simplifies to the mean squared error if only

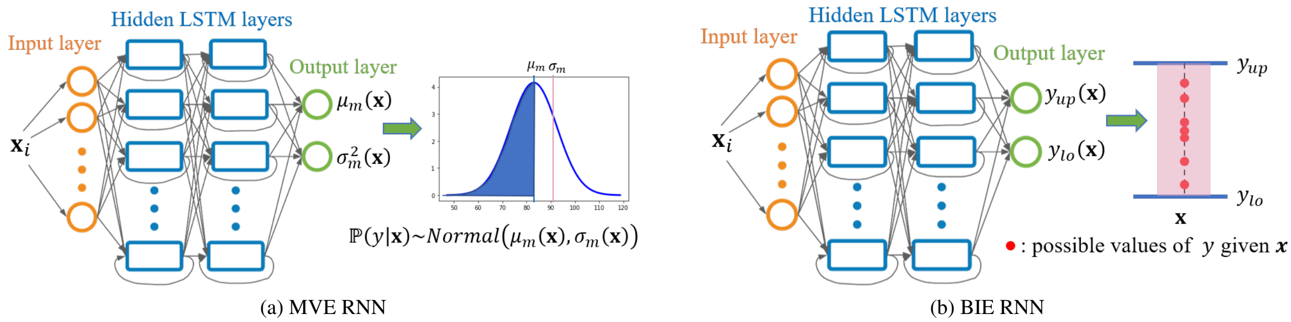

Fig. 2: Stacked LSTM recurrent neural network structures and output. The two networks have the same structure, each with two LSTM hidden layers in sequence, but use different loss functions leading to different output interpretations. For clarity, the full temporal complexities of the blue LSTM units are not shown. The input $\mathbf{x}_i \in \Theta$ is a single input sequence. The units in the first LSTM layer receive the entire input sequence, and return a sequence of outputs to the final LSTM layer which returns only the last hidden state to the output layer.

Table 2: Recurrent neural networks specifications

Parameter	Status
Total number of network layers	4
Input layer output dimension	5
Number of hidden layers	2
Hidden layer output dimension	64 (H1), 32 (H2)
Output layer output dimension	2
Hidden layer type	LSTM (H1), LSTM (H2)
Output layer type	Gaussian (MVE), Dense (BIE)
Objective function (Output)	L_{MVE} (MVE), L_{BIE} (BIE)
Activation function	tanh
Recurrent activation	sigmoid
Bias initialization (BIE)	[-1, 1]
Optimizer	Adam
Learning rate	0.001
Batch size	5096
λ	0.005 (MVE), 0.00025 (BIE)
α (BIE)	0.05

the mean is modeled (i.e. $\sigma^2 = 1$). An ℓ_2 regularization term is added to avoid overfitting.

For BIE, the objective is to minimize the prediction interval while still capturing some minimum portion of the data. This optimization problem can be written in the form shown in Eq.(7).

$$\min_{y_{up,i}(\mathbf{x}_i), y_{lo,i}(\mathbf{x}_i)} \frac{1}{n} \sum_{i=1}^{n} (y_{up,i}(\mathbf{x}_i) - y_{lo,i}(\mathbf{x}_i)) \quad \text{subject to } \frac{c}{n} \geq (1-\alpha) \tag{7}$$

where y_{up} and y_{lo} are the predicted upper and lower bounds output for each input sequence $\mathbf{x}$, n is the number of total data points, c is the number of data points within the prediction interval, and α is a hyperparameter constraining the minimum width of the interval.

To derive a differentiable loss function for BIE from Eq.(7), it is possible to use the Lagrangian multiplier λ and the squared hinge loss to incorporate the constraint. This is possible as the original constraint is equivalent to $\max\left(0, (1-\alpha) - \frac{c}{n}\right) \leq 0$. The resulting loss function is written below in Eq.(8).

$$L_{BIE} = MPIW_{capt.} + \frac{\lambda n}{\alpha(1-\alpha)} \max_{P}(0, (1-\alpha) - P)^2 \tag{8}$$

where $W = MPIW_{capt.}$ is the mean prediction interval width of captured data in Eq.(9), and $P = PICP$ is the prediction interval coverage probability in Eq.(10). In Eq.(6), λ is the regularization coefficient whereas λ in Eq.(8) is a hyperparameter controlling the tradeoff between interval width and coverage, where $(1-\alpha)\%$ is the percentage of points covered by the prediction interval.

$$MPIW_{capt.} = \frac{1}{c} \sum_{i=1}^{n} (y_{up,i} - y_{lo,i}) k_i \tag{9}$$

$$PICP = \frac{c}{n} \tag{10}$$

where k_i enforces that the upper bound is always greater than the lower bound.

4.3 Range & Charging Predictions

Given the mean μ_m and variance σ_m^2 of the predicted SOC required to complete a trip from the MVE RNN, a normal distribution $\mathcal{N}(\mu_m, \sigma_m)$ may be used to determine the probability of finishing the current trip with some minimum state of charge. The cumulative distribution function can be used

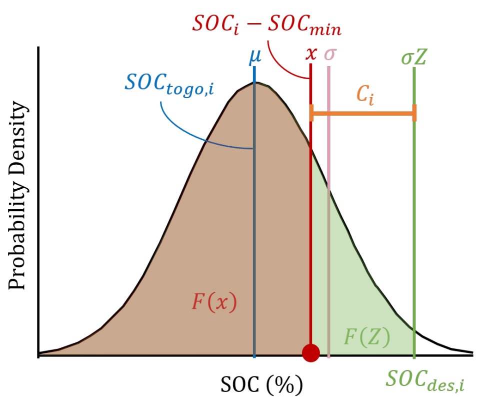

Fig. 3: Toy example of predicted minimum charging required. The cumulative density function for the current SOC minus the specified SOC_{min} is compared with that of the SOC required to ensure some minimum probability β of safely finishing the trip without charging, $SOC_{des,i}$.

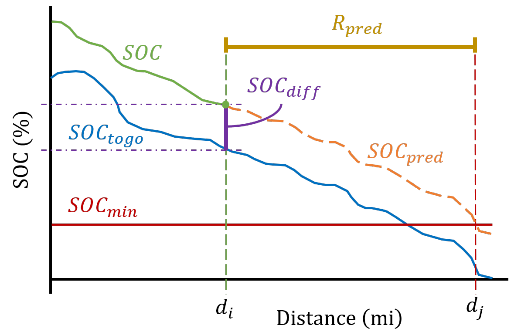

Fig. 4: Toy example of predicted SOC discharge profile and range. The green curve is the real-time SOC up to the current time, while the blue curve is the predicted SOC_{togo} for the trip. This is used to find the predicted future SOC_{pred} for the vehicle. The future point at which this curve falls below the specified SOC_{min} determines the expected range.

to determine the desired probability $\mathbb{P}(\mu \leq x)$, which matches that from Eq.(1) without the charging term. The survival function in Eq.(11), defined as one minus the cumulative distribution function, is the probability that the vehicle will not finish the trip with the desired minimum charge $\mathbb{P}(\mu > x)$. Both functions are defined for any point $x = SOC_i - SOC_{min}$ where $\mu_m = SOC_{togo,i}$ given the μ and σ predicted by either the MVE RNN or BIE RNN. Note that x differs from emboldened $\mathbf{x}$ used in section 4.2.

$$\begin{aligned} S(x;\mu,\sigma) &= \mathbb{P}(\mu > x) = 1 - F(x;\mu,\sigma) \\ F(x;\mu,\sigma) &= \frac{1}{\sigma\sqrt{2\pi}} \int_{-\infty}^{x} \exp - \frac{(t-\mu)^2}{2\sigma^2} dt \end{aligned} \tag{11}$$

Recall that the desired minimum probability to finish a trip without requiring charging in Eq.(1) is a user defined β. The BIE RNN can be used to make conservative estimates without any assumptions about the underlying distribution by simply using the upper-bound output for $\mathbb{E}(SOC_{togo})$ since the BIE RNN produces results using empirical expectations from a certain percentage of the training data. The percentage of capture data is determined by the α parameter since the loss function enforces $(1-\alpha) \leq PICP$. Setting $(1-\alpha) = \beta$ should result in an upper bound that approximates the SOC needed to successfully finish a trip with probability greater than or equal to β. Thus, the expectation of the desired probability from Eq.(11) being greater than β is estimated by using the BIE RNN upper bound output.

$$\mathbb{E}[F(x;\mu,\sigma) \geq \beta] = \mathbb{1}(X \leq x) \tag{12}$$

where $X = SOC_{up,i}$ is the upper bound RNN output and $\mathbb{1}$ is the indicator function.

To approximate the probability of completing the trip using the BIE RNN output, a standard normal distribution $\mathcal{N}(\mu_b, \sigma_b)$ may be assumed between the upper and lower bounds such that the mean $\mu_b = (SOC_{up,i} + SOC_{lo,i})/2$. The variance is determined using the percent point function of the normal distribution $F^{-1}(x)$, which is the inverse of the cumulative distribution function $F(x)$. Given probability $(1-\alpha) = \beta$ for the PICP lower bound, the percent point function returns the z-score $(\pm Z)$ of the upper and lower bound, such that the standard deviation, σ_b is given by Eq.(13) for any point x.

$$\sigma_b = \frac{X - \mu_b}{Z} = \frac{X - \mu_b}{F^{-1}(1 - \frac{\alpha}{2})} \tag{13}$$

Thus, the BIE-predicted probability of finishing the trip above the minimum SOC is obtained by applying Eq.(11) using the BIE mean and standard deviation.

The recommended charge is always the charge needed for $Z = F^{-1}(1 - \frac{\alpha}{2})$, so $SOC_{des,i} = \sigma Z + \mu + SOC_{min}$. Therefore, the recommended minimum charging at each time step is simply $C_i = \max(0, SOC_{des,i} - SOC_i)$. This process for determining the minimum charging C is summarized by Alg.1, and depicted pictorially in Fig.3.

The predicted range of the vehicle is determined by applying Alg.2 based on Eq.(2). The predicted range at each time step $R_{pred,i} = d_j - d_i$ is determined by looking ahead in time for the first index j where $SOC_{pred,j} \leq SOC_{min}$, using the

Algorithm 1 : Charging Requirement Prediction

Input: $SOC, \mu = SOC_{togo}, \sigma, SOC_{min}$
Output: C

```
for each measurement {SOC_i in SOC} do
    P_min(SOC_i − SOC_min ≥ SOC_togo,i) ← β
    Z ← F^{-1}(β + (1−β)/2)
    SOC_des,i ← SOC_togo,i + σZ + SOC_min
    C_i ← max(0, SOC_des,i − SOC_i)
end for
return C, P(SOC − SOC_min ≥ SOC_togo)
```

Algorithm 2 : Trip Range Prediction

Input: $t, d_{rem}, SOC, \mu = SOC_{togo}, SOC_{min}$
Output: R_{pred}

```
for each measurement {SOC_i in SOC_start-to-end} do
    SOC_diff,i ← SOC_i − SOC_togo,i
    for each prediction {SOC_togo,j in SOC_togo,i-to-end} do
        SOC_pred,j ← SOC_diff,i + SOC_togo,j
        if SOC_pred,j ≤ SOC_min then
            break inner for loop
        end if
    end for
    R_pred,i ← d_rem,i − d_rem,j
end for
return R_pred
```

future predicted $SOC_{togo,j}$. An estimate of the remaining trip distance d_{rem} can be used interchangeably with the traveled distance d since $d_{rem,i} = d_{trip} - d_i$. This process is depicted for a single time step in Fig.4.

5 Results

Drive cycle data was collected from a fleet of Class 6 range-extended hybrid trucks operating on actual delivery routes. The raw data contained 75 parameters with significant amounts of missing and incomplete data. Critical parameters such as time, velocity, and GPS location, were collected at a frequency of roughly 0.2 Hz. A sample of similar data was previously published in [42], for which Wang et. al. suggested preprocessing techniques in [43] to effectively use the data for model-based energy estimation. The BEV model described in Section 4.1, based on a fully-electric version of the same Class 6 delivery vehicles, was run assuming zero road inclination using the time and velocity data to estimate the vehicle SOC and trip distance. As in [43], the mean relative error for SOC estimations made using this model was less than 5% for all trips in the study.

Each of the RNN models desribed in Section 4.2 were trained using an input tensor Θ_{train} of size (405152,5,5), with 405152 samples of 5-point sequences with each datapoint containing 5 features. The set of features used was $\{t, d, SOC, La, Lo\}$ where La and Lo are the GPS latitude and longitude measurements, respectively. Additional input features detailing the vehicle performance (e.g. motor speed and torque, mass) and road conditions (e.g. traffic density, number of intersections) may improve performance of similar models if such features are available. A dataset of 112 delivery trips was used, with the two RNN models trained on a set of 52 randomly sampled trips and subsequently tested on 55 other trips. A validation set of 5 trips was reserved to tune hyperparameters, making the final train/validation/test split roughly 45/5/50%. The performance of each model on the training and test trips is summarized in Tab.3. The root-mean-square error (RMSE) of an estimator is the square root of the average squared error between the output of the estimator and the true value estimated parameter. The RMSE for the BIE is measured using the interval mean μ_b. The actual MPIW and PICP for the BIE were computed for all datapoints in the training/test sets. The mean-normalized RMSE (NRMSE), is also reported, and was calculated by dividing the RMSE by the mean of the labeled output SOC_{togo} being predicted. In Tab.3, the RMSE is a measure of percent SOC (as a decimal), and the NRMSE is a normalized percentage (as a decimal).

Table 3: Prediction results for the RNN models

Network	Measure	Result	
		Training	Test
MVE	RMSE	0.052	0.057
BIE	RMSE	0.060	0.054
MVE	NRMSE	0.120	0.133
BIE	NRMSE	0.137	0.124
BIE	MPIW	0.288	0.292
BIE	PICP	0.981	0.996

Fig.5 and Fig.6 show the results from the MVE RNN and BIE RNN, respectively, for a sample trip in which the probability of finishing the trip above the minimum SOC was relatively high and thus the minimum required charging prediction low. Similar results are shown in Fig.A.1 and Fig.A.2 of Appendix A for a trip in which the vehicle did not have sufficient charge to complete the trip.

6 Discussion & Future Works

The results in in Tab.3 demonstrate the strong performance of the RNN models. Although the value of α was set to 0.05 for the BIE RNN, much more than 95% of the data was captured in the prediction interval based on the overall PICP, resulting in slightly more conservative predictions and a MPIW of just over 30%. This implies that the true SOC required to complete a trip varied significantly at each point in time over all of the assessed trips, and yet the mean predictions for SOC_{togo} were quite accurate for both models. The overall RMSE for both RNNs on the entire dataset was within 6%, with little difference between the performance on the test and training sets.

The first example trip chosen is fairly representative of an average trip in which the vehicle is able to safely complete its trip above the minimum $SOC_{min} = 10\%$, finishing with $SOC_{\text{end}} = 16.93\%$. Results for this trip are in Fig.5 and Fig.6. In Fig.5a Fig.6a, there is a clear trend that the models become more certain as the trip nears its end. This is due to the driving patterns of the delivery vehicles, which typically take the same routes back to the depot at the end of a trip. The steep drop in SOC near the trip start and end implies that this set of delivery vehicles typically travel along fast roads when leaving and returning to the depot. Fig.5b and Fig.5c show an inverse correlation between the probability of finishing a trip and the predicted minimum charge required.

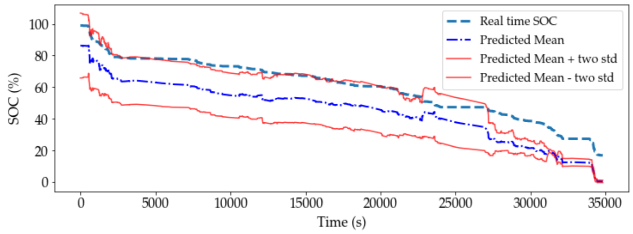

(a) Real-time SOC and predicted SOC_{togo} with confidence bounds

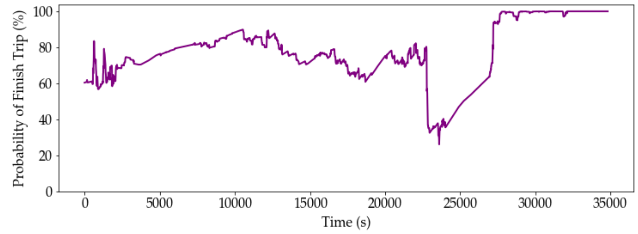

(b) Probability of finishing trip above SOC_{min} without charging

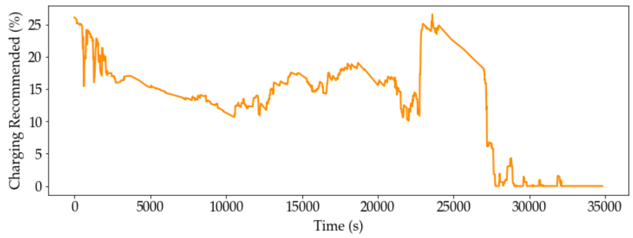

(c) Predicted charging required to increase probability in (b) to β

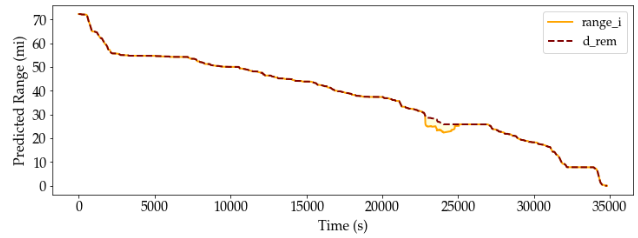

(d) Predicted range lower-bound using MVE-RNN

Fig. 5: Results using MVE RNN on first sample trip

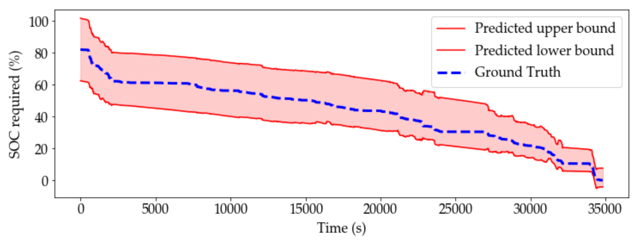

(a) Ground truth SOC_{togo} and predicted SOC_{up} and SOC_{lo} bounds

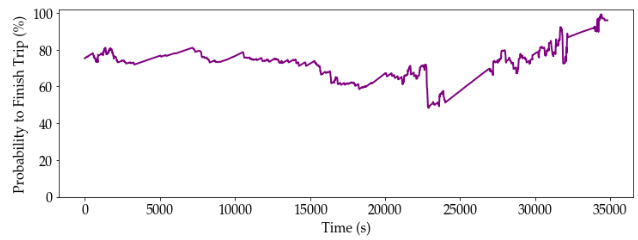

(b) Probability of finishing trip above SOC_{min} without charging

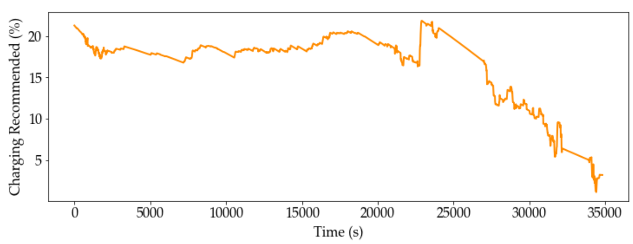

(c) Predicted charging required to increase probability in (b) to $(1-\alpha) = \beta$

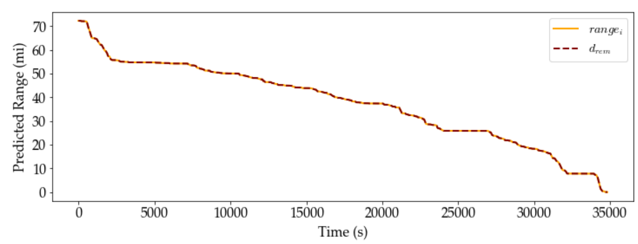

(d) Predicted range lower-bound using BIE-RNN

Fig. 6: Results using BIE RNN on first sample trip

This correlation is similarly shown by Fig.6b and Fig.6c, and is logical given that the probability of finishing the trip considers the vehicle without any charging. As one might expect, the BIE RNN tends to give more conservative and consistent predictions for both the probability of finishing and the charging recommendation, whereas the MVE RNN predictions are much more sensitive to changes throughout an individual trip and sometimes does estimate a higher minimum charging requirement. For the first example trip where the vehicle did not require charging to complete the trip, the MVE RNN finished with a minimum required charging estimate of $C_{\text{end}} = 0\%$ whereas the BIE RNN estimated a required minimum charge of $C_{\text{end}} = 3.18\%$. Although these results show the predictions for required charging converge toward the end of the trip, less conservative models should converge toward final minimum charging requirements more quickly. Both models accurately predicted that the range of the vehicle met or exceeded the remaining trip distance for the majority of the trip, though the MVE RNN briefly underestimated the range around the 25000 second mark in Fig.5d. Future work should include some sensitivity analysis to determine what drive cycle characteristics lead to large output fluctuations.

The second example trip, for which results are shown in Appendix A Fig.A.1 and Fig.A.2, is an example of a trip where the vehicle is unable to finish the trip above 10% SOC, ending with just $SOC_{\text{end}} = 2.35\%$. This corresponds to a trip in which the SOC required is near the upper bound estimate from the BIE RNN as shown in Fig.A.2a. From early on in the trip, both models found it increasingly unlikely that the vehicle would safely complete the trip. This is visible by the low probabilities in Fig.A.1b and Fig.A.2b and the consistently non-zero minimum charging estimations in Fig.A.1c and Fig.A.2c. Additionally, in Fig.A.1d and Fig.A.2d, the predicted range frequently falls below the remaining trip distance from start to end. The required minimum charge at the end of the second trip was predicted to be $C_{\text{end}} = 8.75\%$ by the MVE RNN and a more conservative $C_{\text{end}} = 16.57\%$ by the BIE RNN. In the tested cases, the charging requirements estimated by the two models would indeed allow the vehicles to safely complete the trip, with the BIE RNN typically giving more conservative charging requirement estimates. In cases where the SOC required to complete the trip is near the lower-bound estimate from the BIE RNN, the results tend to look similar to those in Fig.5 and Fig.6, but with the probability of finishing the trip staying very high throughout the trip and the required charging estimate very low.

As seen in the results for both trips, the certainty of each models' predictions improve in parts of each trip with the least variance in historical data, which for the delivery trucks studied is during their return trip at the end of a route. This seems to imply that training the models for specific vehicles could be more effective to best capture unique driving patterns and make the most accurate predictions possible. Similarly, different models could be trained for different types of drive cycles (i.e. highway or city), and/or driver behaviors (i.e. aggressive or passive) to improve the certainty of the predictions in different scenarios. As these results show, having high α and β values cause the BIE and MVE RNNs to be quite conservative in their probability estimates and error on the side of safety, especially at the beginning of the trips. To avoid having high charging requirement predictions at the beginning of trips even when the probability of completing the trip is high, the use of ensemble methods could be explored in the future to train more RNNs with different α and β values. Then, predictions could be biased toward those of less conservative RNN models at the trip start, and more conservative RNN models toward the trip end.

Other possible directions for future work are mentioned in the following section. It is worth noting that to more directly compare alternate approaches for range and minimum charging prediction, some standard benchmarks are needed to better measure the performance of these predictions. This remains a challenge because there are no measurable ground truth values with which to compare the predictions of minimum charge required or remaining range.

7 Conclusions

With the use of BEVs becoming more widespread, range prediction provides key information with which drivers can make informed decisions on when to recharge their vehicles. To help alleviate range anxiety and accommodate BEV owners in a time when charging infrastructure is in its infancy, this work presents a sophisticated approach to model and predict the remaining range and minimum charging requirements for BEVs along a route using recurrent neural networks. Using historical driving data and a tuned vehicle model, labeled input data was generated to train both an MVE and BIE RNN model to predict the energy required to complete a trip with high accuracy, with both models showing less than 6% RMSE, which subsequently provided and estimate of the probability of finish a trip without charging. These predictions then informed the estimation of the minimum charge needed to complete a trip with high probability, and a trip-centric lower-bound on the remaining range for the vehicle.

Planned future work will focus on further exploring the merits of this approach for different use-cases and vehicle classes, with testing done on recent historical data sets not currently presented here. Additional testing is also needed to investigate and optimize the network architecture, for example by deepening the network and using dropout layers between LSTM layers. Further investigation is needed to fully determine the impacts of each hyperparameter for the two loss functions, and their robustness to the introduction of new data. Transferring the networks to adaptive neural networks could improve both the scalability and performance of the models, making it easier to optimize the network structure and to train and update the model weights as new data become available. The use of ensemble methods will also be investigated to see whether the accuracy and consistency of the probability, charging, and range predictions may be improved. The effectiveness of applying the proposed method to each individual vehicle should also be assessed and compared with results for models trained using data from a fleet of vehicles to see how much the model accuracy can improve with decreased variance in driving patterns.

Finally, while this work on parameter estimation can be used to help human drivers if implemented today, the same solution may also be leveraged for decision making in intelligent advanced control systems for autonomous vehicles in the future.

Acknowledgements

This work would not have been possible without the support of the T.E. Murphy Engine Laboratory at the University of Minnesota. The authors would especially like to thank Dr. Pengyue Wang for his guidance and expertise. His previous work on smart energy management systems helped inspire this paper and the research behind it. This material is based upon work supported by the U.S. Department of Energy's Office of Energy Efficiency and Renewable Energy (EERE) under the Vehicle Technologies program, Award Number DE-EE0008805.

constitute or imply its endorsement, recommendation, or favoring by the United States Government or any agency thereof. The views and opinions of authors expressed herein do not necessarily state or reflect those of the United States Government or any agency thereof.

References

[1] Lee, D.-Y., Thomas, V. M., and Brown, M. A., 2013. "Electric urban delivery trucks: Energy use, greenhouse gas emissions, and cost-effectiveness". *Environmental Science & Technology,* **47**(14), pp. 8022–8030. PMID: 23786706.

[2] Stumpf, R., 2019. Americans cite range anxiety, cost as largest barriers for new ev purchases: Study, Feb.

[3] Shaw, N., 2021. Call for better range prediction in electric cars, Mar.

[4] Zhang, B., Sun, X., Liu, S., and Deng, X., 2019. "Recurrent Neural Network-Based Model Predictive Control for Multiple Unmanned Quadrotor Formation Flight". *International Journal of Aerospace Engineering,* **2019**, June, p. e7272387.

[5] Wu, Y., Zhang, Y., Li, G., Shen, J., Chen, Z., and Liu, Y., 2020. "A predictive energy management strategy for multi-mode plug-in hybrid electric vehicles based on multi neural networks". *Energy,* **208**, Oct., p. 118366.

[6] Hu, Q., Amini, M. R., Wiese, A., Seeds, J. B., Kolmanovsky, I., and Sun, J., 2021. "A Multirange Vehicle Speed Prediction With Application to Model Predictive Control-Based Integrated Power and Thermal Management of Connected Hybrid Electric Vehicles". *Journal of Dynamic Systems, Measurement, and Control,* **144**(1), Nov.

[7] Barcellona, S., Grillo, S., and Piegari, L. "A simple battery model for EV range prediction: Theory and experimental validation". In 2016 International Conference on Electrical Systems for Aircraft, Railway, Ship Propulsion and Road Vehicles International Transportation Electrification Conference (ESARS-ITEC), pp. 1–7.

[8] Kessels, J. T. B. A., Rosca, B., Bergveld, H. J., and van den Bosch, P. P. J. "On-line battery identification for electric driving range prediction". In 2011 IEEE Vehicle Power and Propulsion Conference, pp. 1–6. ISSN: 1938-8756.

[9] Sarmiento-Carnevali, M., Fly, A., and Piecha, P. Electric vehicle cold start range estimation through battery-in-loop simulations within a virtual driving environment. ISSN: 0148-7191, 2688-3627.

[10] Hayes, J. G., and Davis, K. "Simplified electric vehicle powertrain model for range and energy consumption based on EPA coast-down parameters and test validation by argonne national lab data on the nissan leaf". In 2014 IEEE Transportation Electrification Conference and Expo (ITEC), pp. 1–6.

[11] Liu, K., Wang, J., Yamamoto, T., and Morikawa, T. "Exploring the interactive effects of ambient temperature and vehicle auxiliary loads on electric vehicle energy consumption". pp. 324–331.

[12] Gebhardt, K., Schau, V., and Rossak, W. R. "Applying stochastic methods for range prediction in e-mobility". In 2015 15th International Conference on Innovations for Community Services (I4CS), pp. 1–4.

[13] Bolovinou, A., Bakas, I., Amditis, A., Mastrandrea, F., and Vinciotti, W. "Online prediction of an electric vehicle remaining range based on regression analysis". In 2014 IEEE International Electric Vehicle Conference (IEVC), pp. 1–8.

[14] Wang, J., Besselink, I., and Nijmeijer, H. "Electric vehicle energy consumption modelling and prediction based on road information". pp. 447–458. Number: 3 Publisher: Multidisciplinary Digital Publishing Institute.

[15] Birrell, S. A., McGordon, A., and Jennings, P. A. "Defining the accuracy of real-world range estimations of an electric vehicle". In 17th International IEEE Conference on Intelligent Transportation Systems (ITSC), pp. 2590–2595. ISSN: 2153-0017.

[16] Varga, B. O., Sagoian, A., and Mariasiu, F. "Prediction of electric vehicle range: A comprehensive review of current issues and challenges". p. 946. Number: 5 Publisher: Multidisciplinary Digital Publishing Institute.

[17] Deepak, S., Amarnath, A., Krishnan U., G., and Kochuvila, S. "Survey on range prediction of electric vehicles". In 2019 Innovations in Power and Advanced Computing Technologies (i-PACT), Vol. 1, pp. 1–7.

[18] Rahimi-Eichi, H., and Chow, M.-Y. "Big-data framework for electric vehicle range estimation". In IECON 2014 - 40th Annual Conference of the IEEE Industrial Electronics Society, pp. 5628–5634. ISSN: 1553-572X.

[19] Conradi, P., Bouteiller, P., and Hanßen, S. "Dynamic cruising range prediction for electric vehicles". In Advanced Microsystems for Automotive Applications 2011, G. Meyer and J. Valldorf, eds., VDI-Buch, Springer, pp. 269–277.

[20] Ferreira, J. C., Monteiro, V. D. F., and Afonso, J. L. "Data mining approach for range prediction of electric vehicle". Accepted: 2012-05-22T14:21:40Z.

[21] De Nunzio, G., and Thibault, L. "Energy-optimal driving range prediction for electric vehicles". In 2017 IEEE Intelligent Vehicles Symposium (IV), pp. 1608–1613.

[22] Vaz, W., Nandi, A. K. R., Landers, R. G., and Koylu, U. O. "Electric vehicle range prediction for constant speed trip using multi-objective optimization". pp. 435–446.

[23] Fukushima, A., Yano, T., Imahara, S., Aisu, H., Shimokawa, Y., and Shibata, Y. "Prediction of energy consumption for new electric vehicle models by machine learning". pp. 1174–1180. Publisher: IET Digital Library.

[24] Gebhard, L., Golab, L., Keshav, S., and de Meer, H. "Range prediction for electric bicycles". In Proceedings of the Seventh International Conference on Future Energy Systems, e-Energy '16, Association for Computing Machinery, pp. 1–11.

[25] Fechtner, H., Teschner, T., and Schmuelling, B. "Range prediction for electric vehicles: Real-time payload detection by tire pressure monitoring". In 2015 IEEE Intelligent Vehicles Symposium (IV), pp. 767–772. ISSN:

1931-0587.

[26] Zhao, L., Yao, W., Wang, Y., and Hu, J. "Machine learning-based method for remaining range prediction of electric vehicles". pp. 212423–212441. Conference Name: IEEE Access.

[27] Wang, Z., Wang, X.-H., Wang, L.-Z., Hu, X.-F., and Fan, W.-H. "Research on electric vehicle (EV) driving range prediction method based on PSO-LSSVM". In 2017 IEEE International Conference on Prognostics and Health Management (ICPHM), pp. 260–265.

[28] Barredo Arrieta, A., Díaz-Rodríguez, N., Del Ser, J., Bennetot, A., Tabik, S., Barbado, A., Garcia, S., Gil-Lopez, S., Molina, D., Benjamins, R., Chatila, R., and Herrera, F., 2020. "Explainable artificial intelligence (xai): Concepts, taxonomies, opportunities and challenges toward responsible ai". *Information Fusion,* **58**, pp. 82–115.

[29] Topić, J., Škugor, B., and Deur, J. "Neural network-based modeling of electric vehicle energy demand and all electric range". p. 1396. Number: 7 Publisher: Multidisciplinary Digital Publishing Institute.

[30] Modi, S., Bhattacharya, J., and Basak, P. "Convolutional neural network–bagged decision tree: a hybrid approach to reduce electric vehicle's driver's range anxiety by estimating energy consumption in real-time". pp. 2399–2416.

[31] Oliva, J. A., Weihrauch, C., and Bertram, T. "Model-based remaining driving range prediction in electric vehicles by using particle filtering and markov chains". In 2013 World Electric Vehicle Symposium and Exhibition (EVS27), pp. 1–10.

[32] Nix, D., and Weigend, A., 1994. "Estimating the mean and variance of the target probability distribution". In Proceedings of 1994 IEEE International Conference on Neural Networks (ICNN'94), IEEE.

[33] Galván, I. M., Valls, J. M., Cervantes, A., and Aler, R., 2017. "Multi-objective evolutionary optimization of prediction intervals for solar energy forecasting with neural networks". *Information Sciences,* **418-419**, Dec., pp. 363–382.

[34] Wan, C., Xu, Z., Pinson, P., Dong, Z. Y., and Wong, K. P., 2014. "Optimal prediction intervals of wind power generation". *IEEE Transactions on Power Systems,* **29**(3), May, pp. 1166–1174.

[35] Hochreiter, S., and Schmidhuber, J., 1997. "Long short-term memory". *Neural Computation,* **9**(8), Nov., pp. 1735–1780.

[36] Pascanu, R., Mikolov, T., and Bengio, Y., 2013. On the difficulty of training recurrent neural networks.

[37] Pascanu, R., Gulcehre, C., Cho, K., and Bengio, Y., 2014. How to construct deep recurrent neural networks.

[38] Graves, A., 2014. Generating sequences with recurrent neural networks.

[39] Graves, A., rahman Mohamed, A., and Hinton, G., 2013. "Speech recognition with deep recurrent neural networks". In 2013 IEEE International Conference on Acoustics, Speech and Signal Processing, IEEE, pp. 6645–6649.

[40] Saleh, K., Hossny, M., and Nahavandi, S., 2017. "Intent prediction of vulnerable road users from motion trajectories using stacked LSTM network". In 2017 IEEE 20th International Conference on Intelligent Transportation Systems (ITSC), IEEE.

[41] Yu, L., Qu, J., Gao, F., and Tian, Y., 2019. "A novel hierarchical algorithm for bearing fault diagnosis based on stacked LSTM". *Shock and Vibration,* **2019**, Jan., pp. 1–10.

[42] Wang, P., 2019. Sample delivery trip data of an extended range electric vehicle.

[43] Wang, P., Li, Y., Shekhar, S., and Northrop, W. F., 2020. A physics model-guided online bayesian framework for energy management of extended range electric delivery vehicles.

Appendix A: Results for Alternate Trip

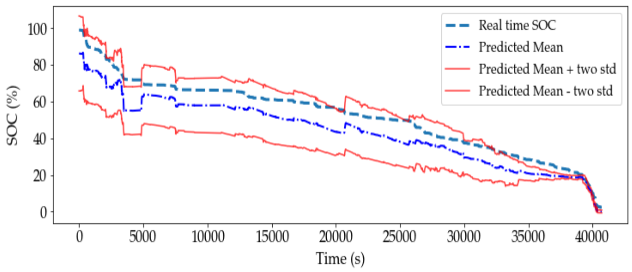

(a) Real-time SOC and predicted SOC_{togo} with confidence bounds

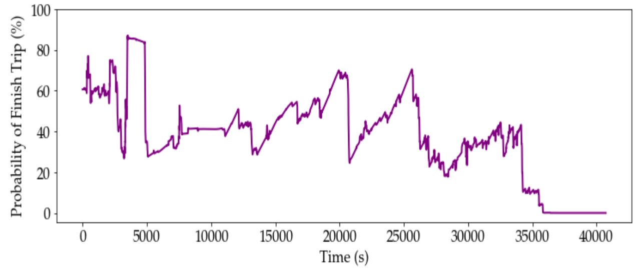

(b) Probability of finishing trip above SOC_{min} without charging

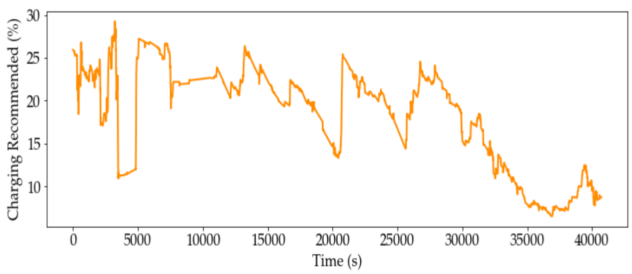

(c) Predicted charging required to increase probability in (b) to $(1-\alpha)=\beta$

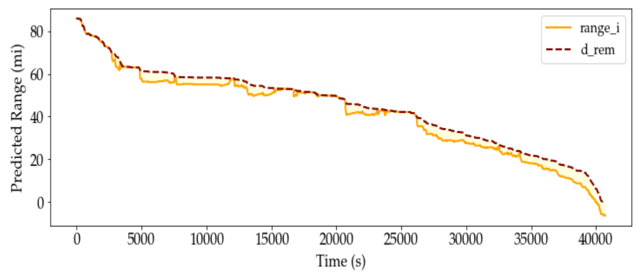

(d) Predicted range lower-bound using MVE-RNN

Fig. A.1: Results using MVE RNN on second sample trip

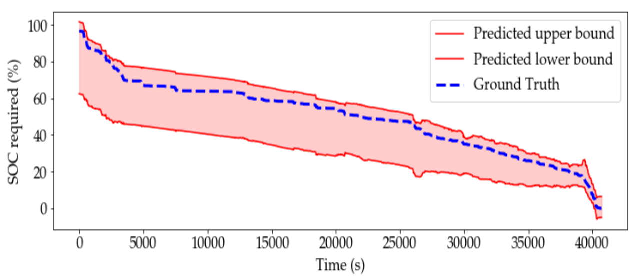

(a) Ground truth SOC_{togo} and predicted SOC_{up} and SOC_{lo} bounds

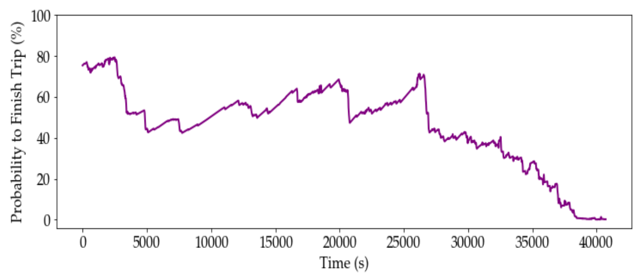

(b) Probability of finishing trip above SOC_{min} without charging

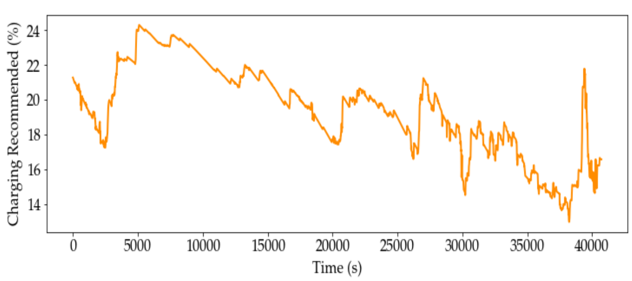

(c) Predicted charging required to increase probability in (b) to $(1-\alpha)=\beta$

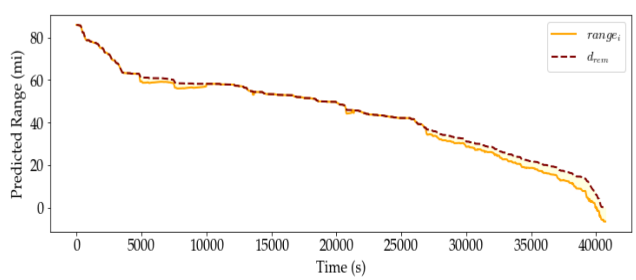

(d) Predicted range lower-bound using BIE-RNN

Fig. A.2: Results using BIE RNN on second sample trip